INVESTIGATION OF THE NEUTRON-ELECTRON INTERACTION

E.L.Enik, L.V.Mitsyna, V.G.Nikolenko, S.S.Parzhitskii, A.B.Popov, G.S.Samosvat, R.V.Khariuzov

Frank Laboratory of Neutron Physics, JINR, Dubna

The problem of refining of the length of the neutron-electron interaction, b_{ne}, remains topical since its existing experimental estimates lie beyond the error limit and also, because it is necessary to know this length to clarify the physical nature of the mean square charge radius of the neutron.

To model more precisely the experiments under preparation to measure b_{ne} from the inelastic scattering of neutrons on a single-atom noble gas, the algorithm describing the angular distribution of neutrons scattered on gas atoms in thermal motion was improved.

The Monte-Carlo calculation of the neutron scattering anisotropy for a "precise" gas sample of argon was repeated and the results were compared with the analytical calculation by the formulas from [1]. The results are illustrated in Fig.1.

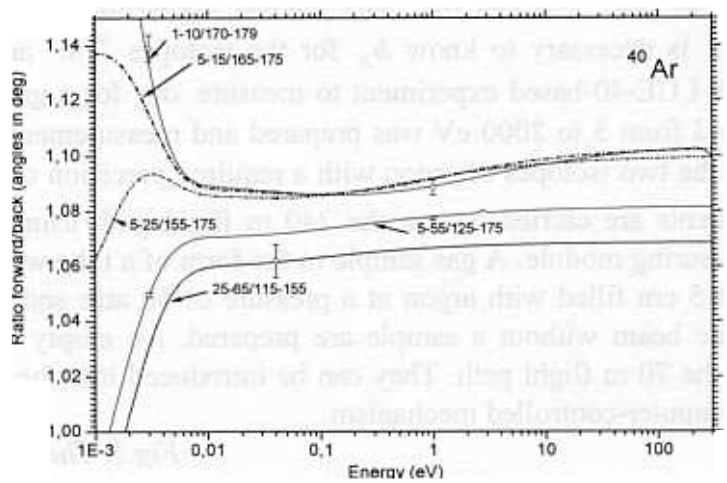

Fig.1. The angular anisotropy of neutron scattering on argon. The curves are the result of analytical calculation for the intervals of forward/backward scattering angles marked with arrows (in degrees). The points represent some variants of the Monte-Carlo calculation.

Figure 1 shows that the analytical and Monte-Carlo calculations agree well and that depending on the value of scattering angles (or their intervals) the effect of the n,e-interaction contribution may reach a value of 1.5%. In addition, an experimental setup with a 5 cm radius neutron beam and a ring detector of ^3He counters (pressure 10 atm and thickness 3 cm) arranged along a radius of 35 cm with respect to the beam axis as illustrated in Fig. 2 was calculated. Figure 3 illustrates the results of the Monte-Carlo calculation for the chosen geometry when a real scattering area from which neutrons come to the detectors has a length of about 90 cm. For comparison, the results of analytical calculations for a "precise" sample and an interval of angles close to the chosen geometry of the setup are presented.

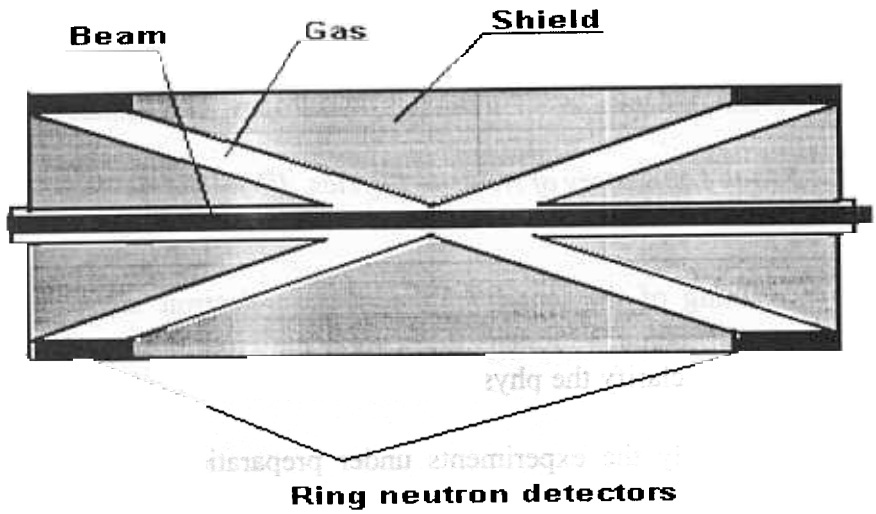

Fig. 2. The scheme of the experimental setup for the measurement of the energy dependence of the angular anisotropy of neutrons scattered on argon.

In the experiment the ratio between n,e- and nuclear scattering-length, b_{ne} / b_N, will be extracted. To obtain b_{ne} it is necessary to know b_N for the isotopes ^{40}Ar and ^{36}Ar present in natural argon. An IBR-30+LUE-40-based experiment to measure σ_{tot} for a gas sample of natural argon in the energy interval from 5 to 2000 eV was prepared and measurements started. This will allow us to obtain b_N for the two isotopes of argon with a required precision using known thermal point data. The measurements are carried out on the 240 m flight path using a battery of ^{3}He counters and a 16-exit measuring module. A gas sample in the form of a tube with a length of about 100 cm and a diameter of 5 cm filled with argon at a pressure of 50 atm and an exact copy of a vacuum tube to imitate the beam without a sample are prepared. An empty and an argon-filled container are installed on the 70 m flight path. They can be introduced into the collimated neutron beam with the help of a computer-controlled mechanism.

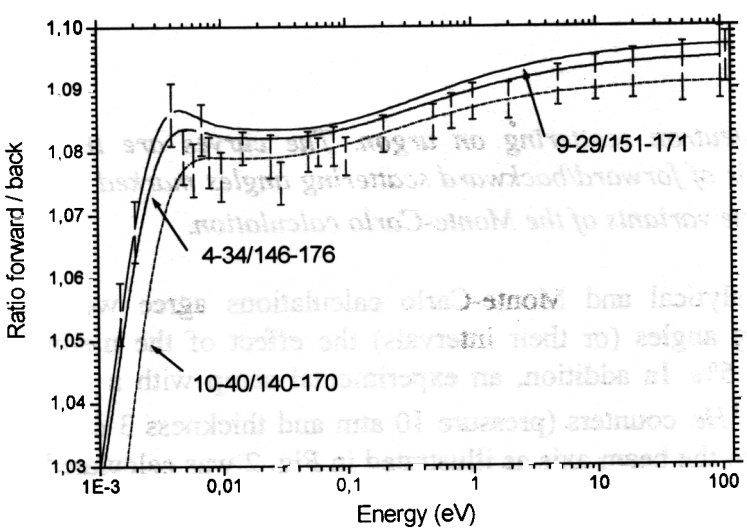

Fig.3. The energy dependence of the angular anisotropy of neutrons scattered on argon. The points are the Monte-Carlo calculation for the setup shown in Fig. 2. The curves are the analytical calculation for realistic intervals of angles for a "precise" sample.

References

1. G.G.Bunatian, V.G.Nikolenko, A.B.Popov, G.S.Samosvat, T.Yu.Tretyakova, Zeit.Phys., **A359**, p.337, 1997.

INVESTIGATION OF INTERFERENCE MINIMA NEAR s-WAVE RESONANCES OF ^{238}U

T.L.Enik, L.V.Mitsyna, G.S.Samosvat *(FLNP, JINR, Dubna, Russia)*
V.V.Sinitsa *(IPPE, Obninsk, Russia)*

1.Introduction

Because of the importance of ^{238}U for nuclear technology, its neutron total and capture cross sections (σ_t and σ_γ respectively) have been measured many times (see, for example [1]). We only know, however, two published works where the scattering cross section σ_s in ^{238}U resonances was studied: in [2] σ_s around the 6.67 eV resonance was only measured and in [3] the scattering resonance area of many resonances was only obtained.

Meanwhile, the interference minima below the resonance energies of s-wave resonances in even-even targets are of a certain interest because very small values of σ_s or the coherent scattering cross section are realized, if the minimum is close to thermal neutron energies (the last phenomenon was observed in [4]).

2.Experiment

Measurements were carried out on a 250.8 m flight path of the Dubna booster IBR-30 using a neutron spectrometer UGRA with a time resolution of ~24 ns/m [5]. A neutron beam with a cross section of 22×12 cm^2 hit a 195 mm diameter of metallic uranium sample depleted with a ^{235}U isotope with a thickness of 3 or 1 mm. The scattered neutrons were detected by two batteries of ^3He-counters which could be set at any of nine positions providing a scattering angle between 25^0 and 155^0 with a $\pm 4^0$ incertainty. The measurement process (choice of the necessary scatterer, angles of detectors, angle between the plane of the scatterer and the beam axis, accumulation of spectra and monitor counts) were made automatically on line with a computer.

3.Analysis

If a nucleous has the neutron scattering cross section $\sigma_s(E)$ at energy E, the yield of the scattered neutrons is:

$$I(E) = p(E)\sigma_s(E)\gamma(E,\alpha,\beta). \qquad (1)$$

Here $p(E)$ includes the neutron flux, detector efficiency and sample dimensions, $\gamma(E,\alpha,\beta)$ is the probability of the neutron entering a flat sample at angle α to a normal experiences scattering and leaves the sample at angle β to a normal. In our case, $p(E)$ depends weakly on E and can be considered as different constants around different resonances. The function $\gamma(E,\alpha,\beta)$ is:

$$\gamma(E,\alpha,\beta)=\begin{cases}\dfrac{1-e^{-nd\left(\frac{\sigma_t}{\cos\alpha}+\frac{\sigma_t'}{\cos\beta}\right)}}{nd\left(\dfrac{\sigma_t}{\cos\alpha}+\dfrac{\sigma_t'}{\cos\beta}\right)} & \textit{for reflection geometry}\\[2ex] \dfrac{e^{\frac{nd\sigma_t'}{\cos\beta}}-e^{\frac{nd\sigma_t}{\cos\alpha}}}{nd\left(\dfrac{\sigma_t}{\cos\alpha}-\dfrac{\sigma_t'}{\cos\beta}\right)} & \textit{for "transmission geometry"}\end{cases}$$

It is obtained by the integration over the sample thickness d. In (2) the total cross sections σ_t and σ_t' correspond to the energy E and $E[(A+\cos\vartheta)/(A+1)]^2$ of the incident and outcoming neutrons, respectively (A is the target mass number and ϑ is the scattering angle). Of course, $\gamma(E,\alpha,\beta)$ is only valid for small $nd\sigma_s$ as it does not take into account multiple scattering.

In order to compare the experimental data with calculations it is necessary to take into account the Doppler and resolution broadening. The first correction was made by means of replacing $I(E)$ in (1) by

$$I^D(E)=\frac{1}{\Delta\sqrt{\pi}}\int_{E-3\Delta}^{E+3\Delta} e^{\left(\frac{E-E'}{\Delta}\right)^2} I(E')dE'$$

with $\Delta=0.0206\sqrt{E}$ eV (E is in eV). The second correction was made by means of replasing $I^D(t)$ being the function of time-of-flight by the weighed average

$$I_R^D(t)=\sum_{i=-7}^{11} I^D(t-i)F(i). \qquad (4)$$

Here, $F(i)$ is normalized time resolution function of the spectrometer, t and i are the integer standing for the 1 mcs channels of the measured spectrum and the histogram $F(i)$. The function (4) plus the constant background B were fitted to the measured spectra in small regions near well isolated resonances by varying the parameters p and B. In (1) the cross section $\sigma_s(E)$ was calculated in the one-level approximation taking into account one or several nearest resonances.

4.Results and discussion

Because of a poor resolution we have chosen to analyse only three low-energy resonances. Raw data for them are partially shown in Fig.1 for two sample thicknesses nd and two scattering angles ϑ. Heavy distortions of the usual resonance form are striking especially for $\vartheta=25^0$ although they are weaker for the sample with nd=0.0048 b^{-1} which was fixed normal to the beam. Due to strong competition with radiative capture the resonance 6.674 eV looks very weak even in comparison with potential scattering. It was hopeless in these conditions to obtain a good fit to the whole resonance with our imperfect correction function $\gamma(E,\alpha,\beta)$ which must be, however, acceptable for describing resonance wings.

The main goal of the discussed investigations is to obtain the experimental values of $\sigma_s(E)$ around the interference minima at $E_{min}=E_0-\Gamma_n/(2k_0R')$. It can be done using equations (1)–(4) but only for the cases when it is possible to neglect multiple scattering, i.e. when $nd\sigma_s/\cos\alpha$ is small. We estimate this conditions for nd=0.0144 b^{-1} and $\alpha=45^0$ as $\sigma_s<15$–20 b which is well fulfilled practically everywhere. So for resonance wings, instead

of (1)–(4) the following spectrum of counts can be used $N_i = C\sigma_{si}\gamma_i + B$, where for each resonance C and B are constants. Then, if we know σ_{sm} at a certain energy E_m corresponding to the channel m, the following takes place:

$$\sigma_{si} = \frac{N_i - B}{N_m - B}\,\frac{\gamma_m}{\gamma_i}\,\sigma_{sm} \qquad (5)$$

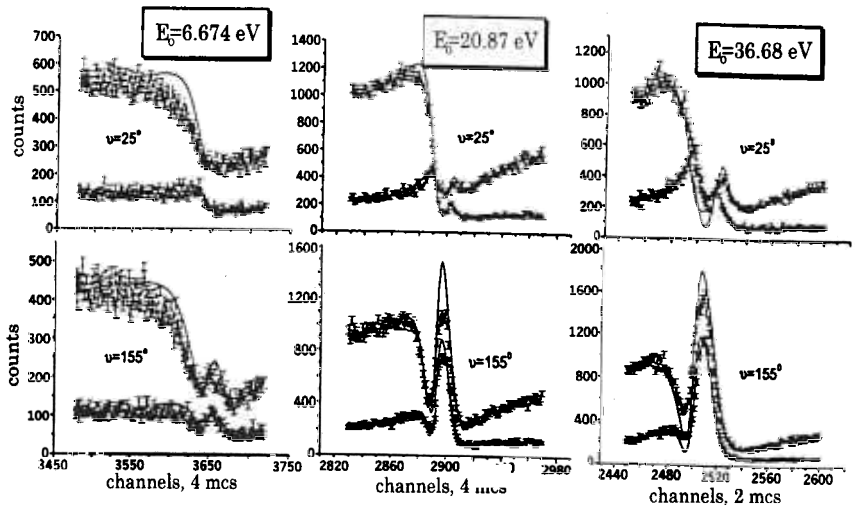

Fig.1. The time-of-flight spectra of neutrons scattered by ^{238}U. Upper spectrum in each diagram relates to the sample with nd=0.0144 b^{-1} and α=45° (120 hours of running), lower spectrum relates to nd=0.0048 b^{-1} and α=0° (96 hours of running). Solid lines are the fits to the wings (30–50 channels left and 50–80 channels right)

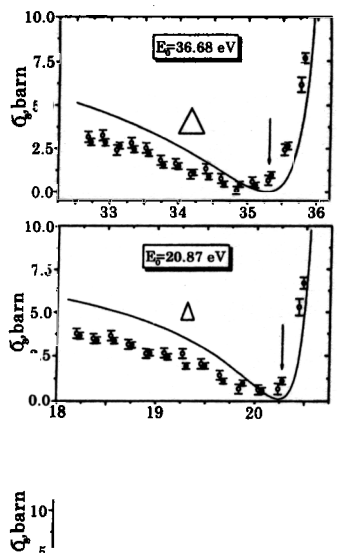

Three values of E_m on the high-energy wings of resonances are chosen and the cross sections σ_{sm} are obtained for them from the well-known file JENDL-3. The values of both quantities are presented in the table. This gives us the possibility to achieve the declared aim using formula (5). The results are shown in Fig.2. The base of each triangle is a double half-width of the local energetic resolution and the arrows indicate the theoretical position E_{min} (without Doppler effect) of the σ_s minima. The solid lines are the calculated results from the file JENDL-3. The squares for the 6.674 eV resonance are our rough estimation of the result [2]. Fig.2 allows us to say that the

Fig.2. The scattering cross sections near the resonances. Black points relate to the ϑ=155° measurements, light points relate to the ϑ=90° measurements

E_0, eV	E_{min}, eV	E_m, eV	σ_{sm}, b
6.674	6.525	8.05	11.2
20.87	20.28	23.05	14.2
36.68	5.29	39.50	23.7

measured and calculated σ_s are in moderate agreement. Some difference can be explained, besides the finite resolution of the setup, by any possible inaccuracies in the obtaining both results.

References

[1] D.K.Olsen, G.de Saussure, R.B.Perez, E.G.Silver, F.C.Difilippo, R.W.Ingle, H.Weaver. Nucl. Sci. Eng., 1977, v.62, p.479.

[2] P.Stavelov, F.Poortmans, L.Mewissen, E.Cornelis. Nucl. Sci. Eng., 1978, v.66, p.349.

[3] M.Asghar, C.M.Chaffey, M.C.Moxon. Nucl. Phys., 1966, v.85, p.305.

[4] Yu.A.Alexandrov. JINR 3-3442, p.112, Dubna, 1967 (in Russian).

[5] B.I.Voronov, T.L.Enik, V.A.Ermakov, V.I.Konstantinov, E.I.Litvinenko, L.V.Mitsyna, G.S.Samosvat, A.A.Smirnov, V.A.Trepalin, R.V.Kharjuzov. JINR Communication P13-97-36, Dubna, 1997 (in Russian); T.L.Enik, R.V.Kharjuzov, L.V.Mitsyna, G.S.Samosvat. Nucl. Instr.Meth., 2000, v.A440, p.777.

PARITY VIOLATION AND INTERFERENCE EFFECTS IN ANGULAR DISTRIBUTIONS OF FISSION FRAGMENTS

V.P. Alfimenkov, N.A.Bazhanov, L.Lason[1], Yu.D.Mareev, V.V.Novitskii, L.B.Pikelner, T.L.Pikelner, M.I.Tsulaia, A.N.Chernikov

Frank Laboratory of Neutron Physics, JINR, Dubna
[1]Lodz University, Poland

In the year 2000 investigations of the parity violation and interference effects in the angular distributions of fragments of the resonance neutron induced fission of heavy nuclei continued.

The angular correlations in resonance neutron induced fission can be written as

$$W(\mathbf{P}_f) = 1 + \alpha_{pv}(\sigma_n \cdot \mathbf{P}_f) + \alpha_{fb}(\mathbf{P}_f \cdot \mathbf{P}_n) + \alpha_{lr}(\mathbf{P}_f \cdot [\sigma_n \cdot \mathbf{P}_n]),$$

where $\mathbf{P}_f$ and $\mathbf{P}_n$ are the unit vectors of the momentums of the light fission fragments and neutrons that caused the fission, σ_n is the unit pseudovector in the direction of neutron polarization. The coefficients α_{pv}, α_{fb}, and α_{lr} characterize respectively the effects of parity violation, forward-backward and left-right asymmetry in the emission of the fragments. There exist theories [1, 2] describing these coefficients as a function of the parameters of s- and p-wave resonances and also, of the matrix elements of the weak interaction for the coefficient α_{pv}. The experimental investigations of the reported effects over the region of resonance energies were conducted by joint groups of PINP (Gatchina) and FLNP JINR (Dubna) in the recent years. The generalized results of the investigations of all the effects for ^{235}U are published in [3] and the experiments with ^{233}U nuclei completed in 1999 are described in [4]. In 2000, measurements of ^{239}Pu were carried out.

One of the specific features of the transverse cross section of fission and radiative neutron capture in ^{233}U and ^{235}U nuclei is a high density of neutron resonances and a small number of reduced neutron widths. For s-resonances the average spacing between resonances is about 0.5 eV and the average reduced widths is about 10^{-4} eV. These two facts make it almost impossible to observe directly p-wave resonances in which the existence of the cetrifugal barrier results in that the cross section of compound state formation in the area of 10 eV neutron energy is smaller than in s-wave resonances 4 – 5 orders of magnitude. Parallel investigations of the above-mentioned effects make it possible to determine the positions of unknown p-resonances and do the assessment of their main parameters. Figure 1 depicts the energy behavior of all three effects over the neutron energy range from thermal to 15 eV for ^{233}U. A distinctly seen structure of the effects (fb) and (lr) has made it possible to determine the parameters of 18 p- resonances. As it is seen in Fig. 1 the parity violation effects are noticeably weaker. However, we managed to assess the value of three matrix elements. The obtained values lie in the interval from 10^{-4} to 10^{-3} eV.

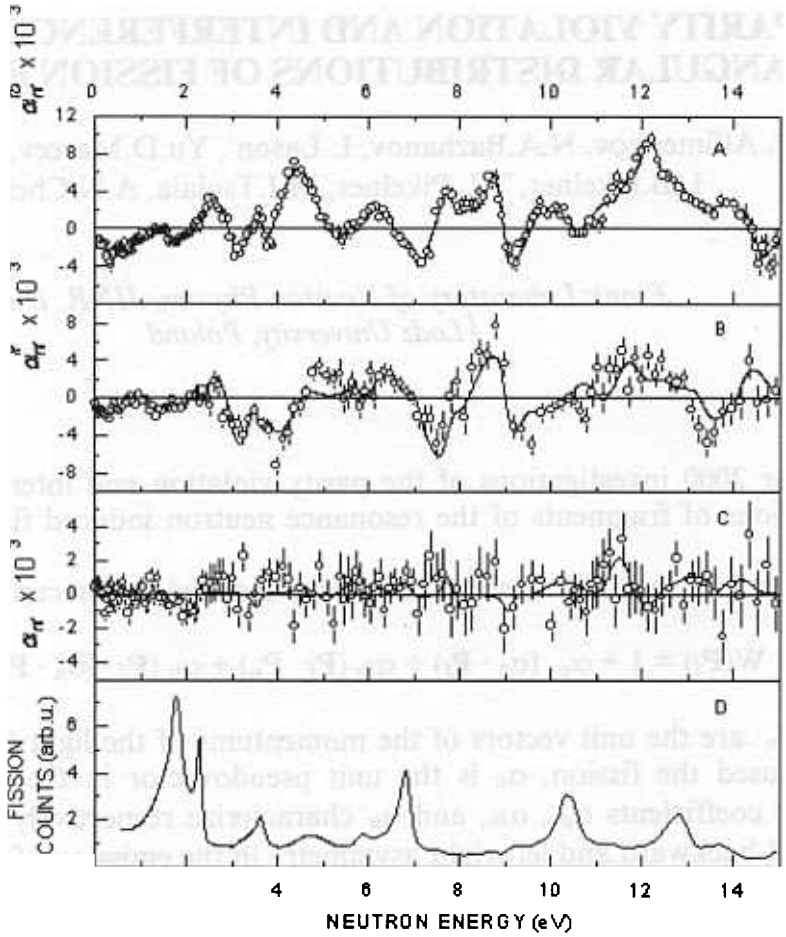

Fig. 1.

The measurements of ^{239}Pu started in 1999 and continued through the year 2000 have their pluses and minuses. The positive side is that it has a noticeably smaller density of levels than uranium isotopes. The average distance between resonances is 2.3 eV. This simplifies joint processing of the obtained spectra because the contribution of neighboring resonances to the analyzed section decreases. At the same time, however, it leads to a decrease in the effect that depends on the distance between the mixing levels. In this connection in the year 2000, we continued to collect statistics on the measurement of the left-right asymmetry and parity violation in the resonance neutron-induced fission of ^{239}Pu with the POLIANA facility at the IBR-30 reactor.

References

[1] Sushkov O.P., Flambaum V.V., Usp.Fiz.Nauk, 1982, v. 136, p. 3.
[2] Bunakov V.E., Gudkov V.P., Nucl. Phys., 1983, v.A 401, p.93.
[3] Alfimenkov V.P.,Chernikov A.N., Lason L. et al. Nucl. Phys., 1999, v.A645, p. 31.
[4] Alfimenkov V.P., Gagarskii A.M., Golosovskaia S.P. et al., Jad.Fiz, 2000, v.63, p.598.

Improving Explosive Nucleosynthesis Models Via (n,α) Measurements

P. E. Koehler[1], Yu. M. Gledenov[2], J. Andrzejewski[3], K. H. Guber[4], S. Raman[1], T. Rauscher[5]

[1] *Physics Division, Oak Ridge National Laboratory, Oak Ridge, Tennessee 37831*
[2] *Frank Laboratory of Neutron Physics, Joint Institute for Nuclear Research, 141980 Dubna, Russia*
[3] *Department of Nuclear Physics and Radiation Safety, University of Lodz, 90-236 Lodz, Pomorska St. 149, Poland*
[4] *Computational Physics and Engineering Division, Oak Ridge National Laboratory, Oak Ridge, TN 37831*
[5] *Departement für Physik und Astronomie,Universität Basel, CH-4056 Basel, Switzerland*

Recently, there has been much interest [1-5] in the astrophysical rates for reactions between α particles and intermediate to heavy nuclei. These reactions often can play an important role in the nucleosynthesis occurring in massive stars at high temperatures and in explosive scenarios such as supernovae. For example, photodisintegration processes such as (γ,α) reactions play an essential role in the nucleosynthesis of the proton-rich intermediate to heavy elements in the so-called *p*-process [6,7]. A better understanding of the nucleosynthesis occurring in these environments should lead to improved stellar models and impact related areas such as the origin of isotopic anomalies in meteorites [1]. Possible *p*-process contributions to s-only isotopes are also relevant for high-precision tests of *s*-process models [8]. There is scant experimental information on the rates for these reactions and the few data which have been measured are sometimes very different from theoretical predictions. Direct determinations of these rates via experiments are extremely difficult and it is very unlikely that the rates for most of the needed reactions will be determined by direct experiments. Theoretical calculations are hampered by large uncertainties in the α+nucleus optical potential in the astrophysically relevant energy range. Traditional methods for improving optical potentials, such as elastic scattering of α particles [9], have been of limited usefulness because the potentials must be extrapolated from measurements made at energies well above the astrophysically interesting range. A series of low-energy (n,α) cross-section measurements may offer the best opportunity for enabling global improvements in the α+nucleus optical potential for astrophysics applications because; i) the Q-values for (n,α) reactions are such that the relative energy between the α particle and the residual nucleus are in the astrophysically interesting range, so no extrapolation is necessary; ii) scaling the sample size to that employed in a previous measurement [10] using predicted cross sections [11], we calculate that as many as 30 nuclides across a wide range of masses should be accessible to measurements, and iii) a recent study [3] has shown that calculated (α,n) rates, via the α transmission coefficients, are sensitive to the α-potential used in the model. By detailed balance arguments, (n,α) reactions should display the same sensitivity. The data presented herein are the first (n,α) cross section measurements in this mass range over the broad range of energies of interest to

nuclear astrophysics. It is intended that they represent the first in a series of measurements aimed at a global improvement in the calculation of rates for α-induced reactions of interest to explosive nucleosynthesis models.

The experiments were performed at the Oak Ridge Electron Linear Accelerator (ORELA) white neutron source. The ORELA was operated at a repetition rate of 525 Hz, a power of 6 - 8 kW and a pulse width of 8 ns. A compensated ionization chamber (CIC) [10] was used as the detector. Although a CIC can have poorer pulse-height resolution than, for example, a gridded ionization chamber, it reduces γ flash effects by several orders of magnitude, allowing measurements to be made to much higher neutron energies (500 keV in the present case) than in previous experiments [12]. The source-to-sample distance was 8.835 m and the neutron beam was collimated to 10 cm in diameter at the sample position. The $^{6}Li(n,\alpha)^{3}H$ reaction was used to measure the energy dependence of the flux and to normalize the raw counts to absolute cross section. The data for ^{147}Sm [13] in the unresolved region are shown in Fig. 1, together with cross sections calculated by three statistical model codes [11,14,15] frequently used for astrophysical applications. The theoretical cross sections are renormalized by the constant factors given in the figure. The older calculations of Ref. [11] are much closer to the data than the more recent calculations of Refs. [14,15] which are roughly a factor of 3 different from the data in opposite directions. The comparison to our new data provides important clues to problems with the α potentials in the models.

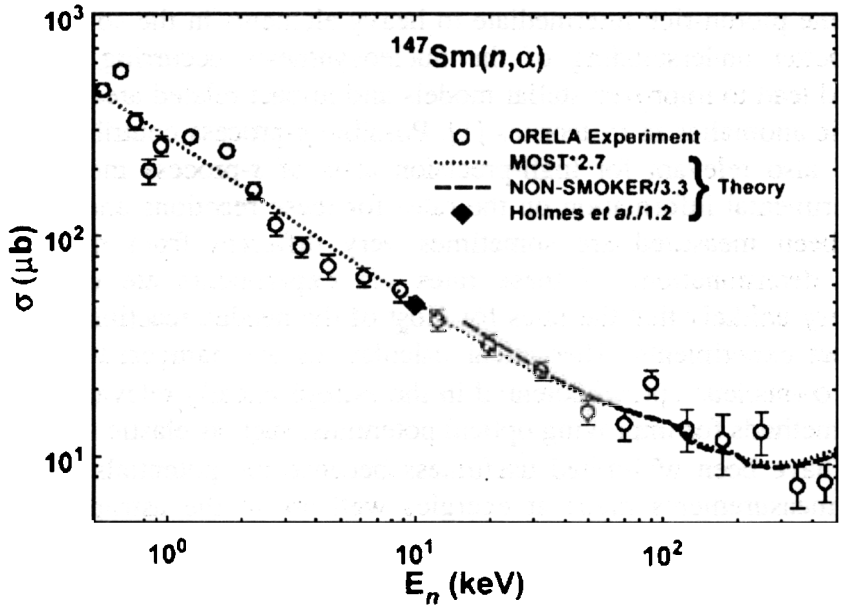

Fig.1. Cross sections for the ^{147}Sm (n,α) reactions in the unresolved region. Shown are the measurements of the present work (circles with error bars depicting one-standard-deviation statistical uncertainties) and calculations by Holmes et al. [11] (diamonds), as well as calculations using the newer statistical model codes NON-SMOKER [14] (long-dashed curves), and MOST [15] (dotted curves).

We studied theoretically [13] the dependence of the calculated ^{147}Sm (n,α) reaction rates on the optical α potential as well as the nuclear level density. The NON-SMOKER [14] code was used to calculate the astrophysical reaction rates

^{147}Sm (n,α) using two different optical α+ nucleus potentials and three different level density prescriptions, in addition to the standard NON-SMOKER potential and level density. Differences of about a factor of 30 can be accounted for in the variation of the optical potential alone. The different level density prescriptions can change the cross section by a factor of about 1.5, by far smaller than the effect of the α potential. However, we want to emphasize that this is not a systematic study of the sensitivity but merely presented to illuminate the source of the differences in the results from various statistical model calculations. Although it is possible to obtain an α potential by fitting the current experimental data, such a potential probably would be of limited usefulness. For example, it has recently been shown [5] that a potential constructed to give good agreement with the experimental data for the ^{144}Sm (α,γ) reaction can be off by as much as a factor of 100 compared to the data for the ^{70}Ge(α,γ) reaction. More experimental data are needed across as wide a range of masses and energies as possible to constrain the several parameters thought to be needed to define a global α potential. The proper treatment of the statistical model of nuclear reactions involving α particles poses a very important problem in nuclear astrophysics today. It is especially crucial for a better understanding of the nucleosynthesis occurring in stellar explosions such as supernovae and the origin of the *p*- nuclides. We have demonstrated the feasibility of a new approach for reducing the main uncertainty in the calculation of rates for reactions involving α particles. It is evident that further experimental data of the type presented herein are needed to more fully explore this problem if the statistical model and the explosive nucleosynthesis calculations which in large part rely on them are to be improved.

References

1. S. E. Woosley and W. M. Howard, Astrophys. J. Lett. **354**, (1990) L21.

2. T. Rauscher, F. -K. Thielemann, and H. Oberhummer, Astrophys. J. Lett. **451**, (1995) L37.

3. R. D. Hoffman, S. E. Woosley, T. A. Weaver, T. Rauscher, and F.-K. Thieleman, Astrophys. J. **521**, (1999) 735.

4. T. Rauscher, in Nuclei in the Cosmos, edited by N. Prantzos and S. Harissopulos (Editions Frontieres, Gif-sur-Yvett, 1998), p. 484.

5. E. Somorjai, Zs. Fulop, A. Z. Kiss, C. E. Rolfs, H.-P. Trautvetter, U. Greife, M. Junker, M. Arnould, M. Rayet, S. Goriely, T. Rauscher, H. Oberhummer, and P. Mohr, Astron. Astrophys. **333**, (1998) 1112.

6. S. E. Woosley and W. M. Howard, Astrophys. J., Suppl. **36**, (1978) 285.

7. M. Rayet, M. Arnould, M. Hashimoto, N. Prantzos, and K. Nomoto, Astron. Astrophys. **298**, (1995) 517.

8. K. H. Guber, R. R. Spencer, P.E. Koehler, and R. R. Winters, Phys. Rev. Lett. **78**, (1997) 2704.

9. P. Mohr, T. Rauscher, H. Oberhummer, Z. Mate, Z. Fulop, E.Somorjai, M. Jaeger, and G. Staudt, Phys. Rev. C **55**, (1997) 1523.

10. P.E. Koehler, J.A. Harvey, and N.W. Hill, Nucl. Instr. and Meth. **A361**, (1995) 270.

11. J.A. Holmes, S.E. Woosley, W.A. Fowler, and B.A.Zimmerman, At. Data Nucl. Data Tables **18**, (1976) 305.

12. J. Kvitek and Y. P. Popov, Nucl. Phys. **A154**, (1970) 177.

13. Yu. M. Gledenov, P. E. Koehler, J. Andrzejewski, K. H. Guber, and T. Rauscher, Phys. Rev. **C 62** (2000) 042801(R).

14. T. Rauscher and F.-K. Thielemann, in Stellar Evolution, Stellar Explosions, and Galactic Chemical Evolution, edited by A. Mezzacappa (Institute of Physics, Bristol, 1998), p.519.

15. S. Goriely, in Nuclei in the Cosmos, edited by N. Prantzos and S. Harissopulos Editions Frontieres, Gif-sur-Yvette, 1998), p. 314.

Level density and radiative strength functions of dipole transitions below B_n in $^{185,187}W$ and $^{191,193}Os$

V.A.Bondarenko[a], J.Honzátko[b], V.A. Khitrov[c], A.M. Sukhovoj[c], I.Tomandl[b]
[a] *Nuclear Research Center, LV 2169 Salaspils, Latvia*
[b] *Nuclear Physics Institute, CZ-25068 Řež near Prague, Czech Republic*
[c] *Frank Laboratory of Neutron Physics, Joint Institute for Nuclear Research 141980 Dubna, Russia*

1 Introduction

Information on the properties of the excited states of heavy non-magic nuclei for the excitation region from 1-3 MeV to the neutron binding energy, B_n, can be derived from an analysis of the energy dependence of the level density, ρ, and reduced probability (strength function) f of their excitation after the decay of compound states. Up to now, there have been no methods which would allow the determination of these parameters without some additional information (for example, model assumptions with an unknown precision). Therefore, main information on the level density was obtained [1] from analyses of the products of nuclear reactions with the use of different potentials of the optic model to predict an unknown probability of nucleon emission with further excitation of an arbitrary low-lying level. New possibilities are provided by the investigation of two-step γ-cascades between the neutron resonance and given low-lying levels.

Unlike other compound nucleus reaction with yields proportional to the level density, the intensity of two-step γ-cascades (to one or several final levels) is, on the whole, inversely proportional to the level density of the nucleus. Theoretically there is an infinite number of possible ρ and f values which provide precise reproduction of experimental cascade intensities and total radiative widths of neutron resonances. However, due to a unique property of this experiment, the interval of probable estimates of ρ and f is limited by certain minimum and maximum values for all excitation energies of the nucleus. As it was shown in [2], these intervals are narrow enough in order to verify different models of nucleus. This is the main difference of the data used below from, for instance, that on spectra of primary γ-transitions where the interval of theoretically possible values is always infinite. It is obvious that analysis by the method [2] requires experimental cascade intensities with sufficiently small statistic and systematic errors.

2 Experimental data

Two-step γ-cascades following thermal neutron capture in the $^{184,186}W$ and $^{190,192}Os$ target nuclei were measured at the Light-Water Reactor LWR-15 in Řež near Prague. The $\gamma-\gamma$ coincidences were measured [3] with $HPGe$ detectors of sufficiently enough efficiency, which enabled us to achieve 5 to 10 times higher statistics than in earlier experiments in Dubna and Riga. This allowed us to obtain the spectra where up to 80-90% of cascade intensities are resolved as pairs of peaks, i. e., the main portion of the experimental intensity can be related to quite defined cascades which excite individual intermediate levels and can be analysed using the technique of nuclear spectroscopy. The use of the algorithm [4] for the determination of quanta ordering in the resolved cascades allowed us to estimate [5] the dependence of the cascade intensity on the energy of their intermediate levels (Fig. 1).

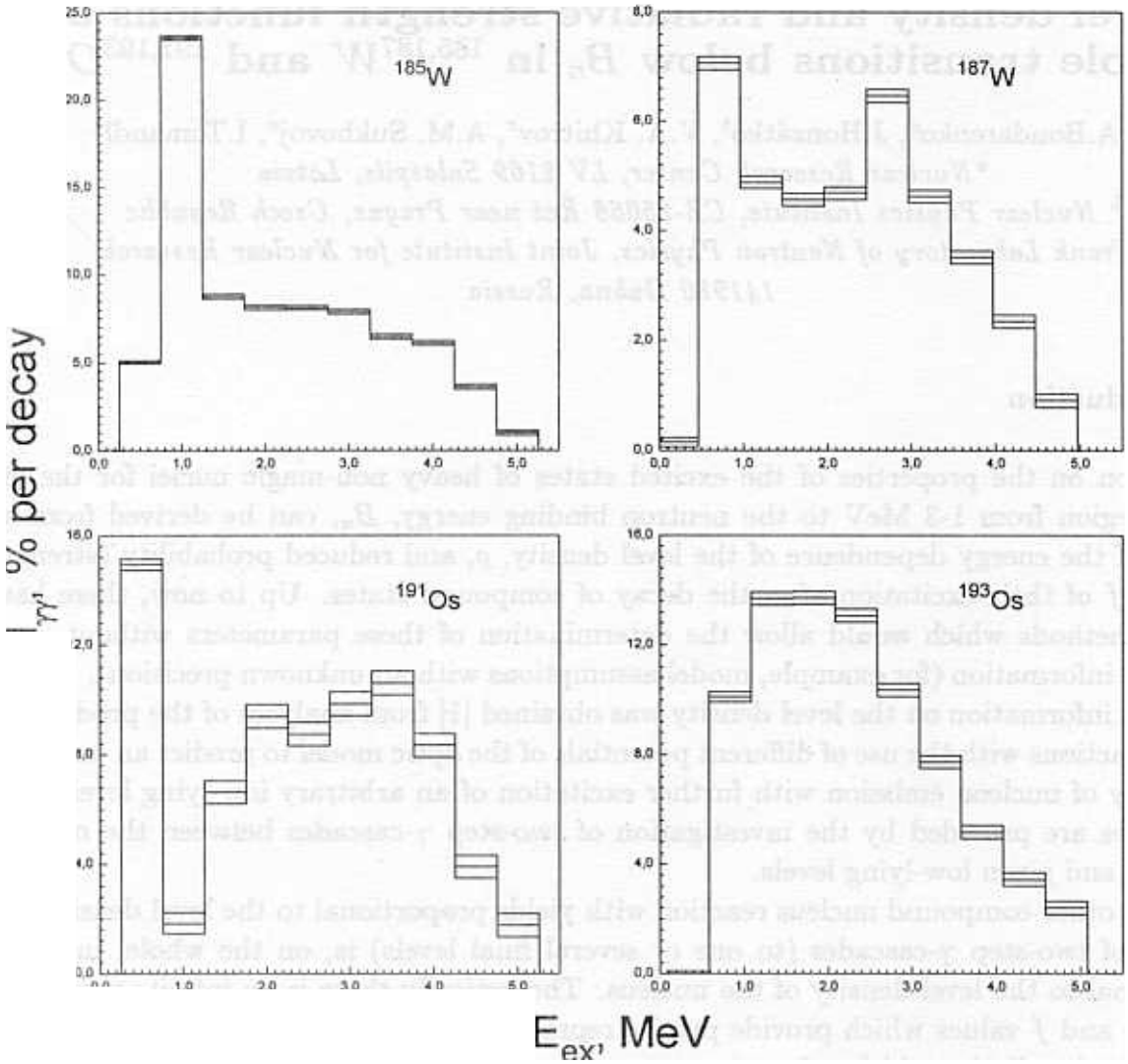

Fig. 1. The total experimental intensities (in % per decay) of two- step cascades (summed in energy bins of 500 keV) with ordinary statistical errors as a function of the primary transition energy.

Most probably, systematic error of this result does not exceed [6] 5-10%.

Specific dependence of the cascade intensities on the density ρ of their intermediate levels and radiative strength functions f of cascade transitions in conjunction with the known total radiative strength function of the capture state allow the determination [2] of the probable interval of ρ and f values. The corresponding results are shown in Figs. 2 and 3. intermediate levels per 100 keV observed earlier. As it is described in [2], the "best" values and intervals of their probable variations (which allow the reproduction of the experimental intensities (Fig. 1) within the precision of the experiment) are determined here as a mean value and dispersion of ensembles of random ρ and f obtained in Monte-Carlo simulations. A simple iterative algorithm was used for this purpose: we set some different initial values for the level density and partial radiative widths and then distorted them by means of random functions. If these distortions improve the agreement between the experimental and calculated cascade intensities and total radiative widths of the capture state at this stage of the iterative procedure, then the distorted values are used as initial parameters in the next iteration. Repeated iterative calculations for the W and Os isotopes and the nuclei studied earlier [2]

leads to convergent in probability of "best" values independently on the initial ρ and f values in the realized random process.

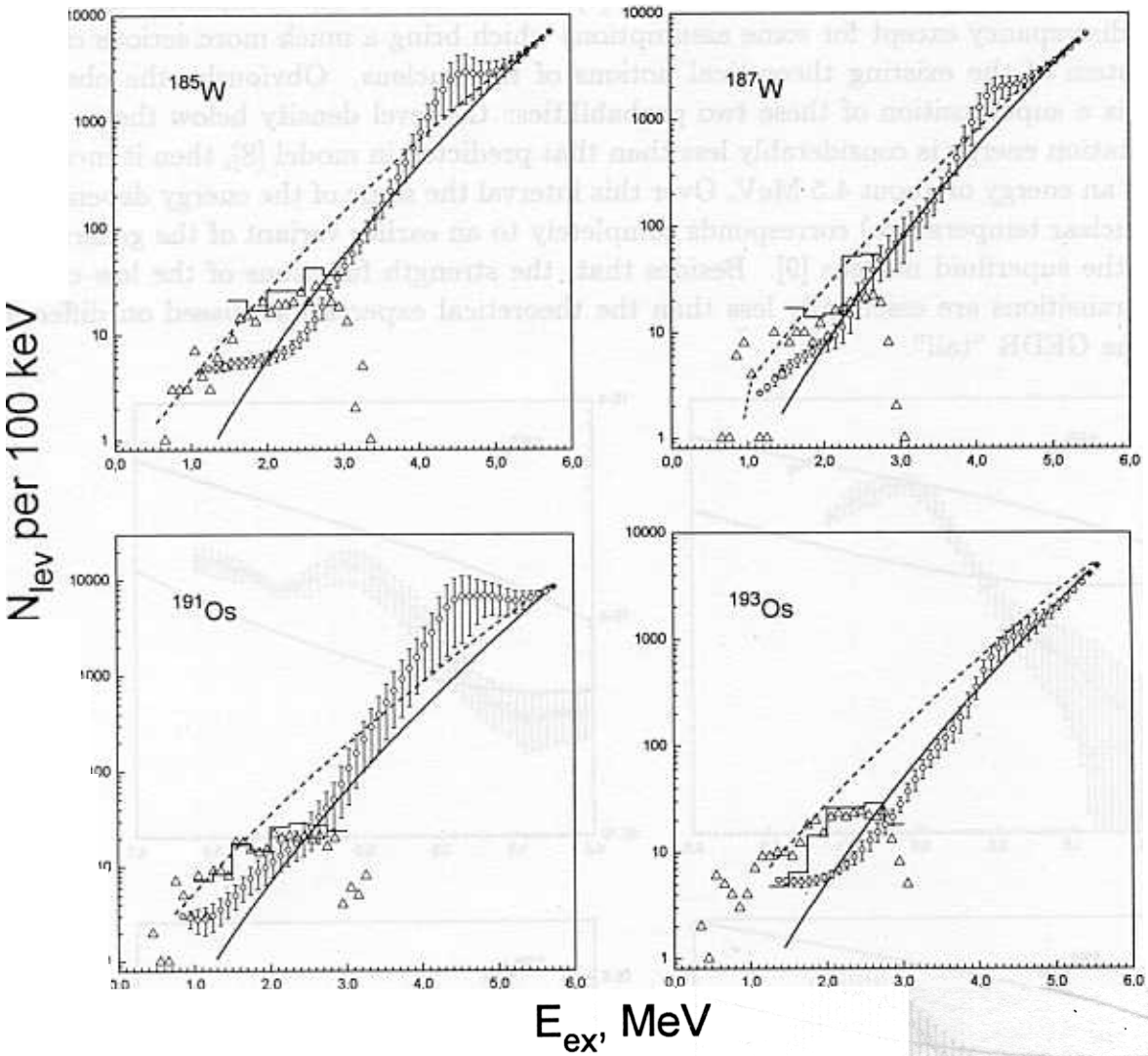

Fig. 2. The interval of probable values of the level density enabling the reproduction of the experimental intensity of two-step cascades and total radiative widths of capture states in $^{184,186}W$ and $^{190,192}Os$. The dashed and solid lines represent the predictions [8] and [9], respectively. The histogram represents the data [6], triangles show the number of cascade intermediate levels per 100 keV observed earlier.

Even-odd nuclei with $A > 180$ are characterized by considerable local fluctuations of the intensities of primary transitions to low-lying levels. This circumstance and the necessity to average the cascade intensities (Fig. 1) over the 0.5 MeV energy interval lead to "breaking" of the strength functions in Fig. 3.

3 Possible interpretation of the results of analysis

The experimental intensities of two-step cascades in $^{185,187}W$ and $^{191,193}Os$ are noticeably larger than the theoretical values calculated according to the models of level density and radiative strength functions which consider nucleus as a Fermi-liquid [7] or Fermi-gas [8]. This

means that the level density excited in the (n,γ) reaction is considerably less than the predicted in the model [8] or that the dependence of the strength function f on the γ-transition energy is much stronger than it follows from [7]. There are no other explanations of the observed discrepancy except for some assumptions which bring a much more serious change in the system of the existing theoretical notions of the nucleus. Obviously, the observed situation is a superposition of these two probabilities: the level density below the $\simeq 2-3$ MeV excitation energy is considerably less than that predicted in model [8], then it increases rapidly to an energy of about 4.5 MeV. Over this interval the slope of the energy dependence (due to nuclear temperature) corresponds completely to an earlier variant of the generalized model of the superfluid nucleus [9]. Besides that, the strength functions of the low-energy primary transitions are essentially less than the theoretical expectations based on different ideas of the GEDR "tail".

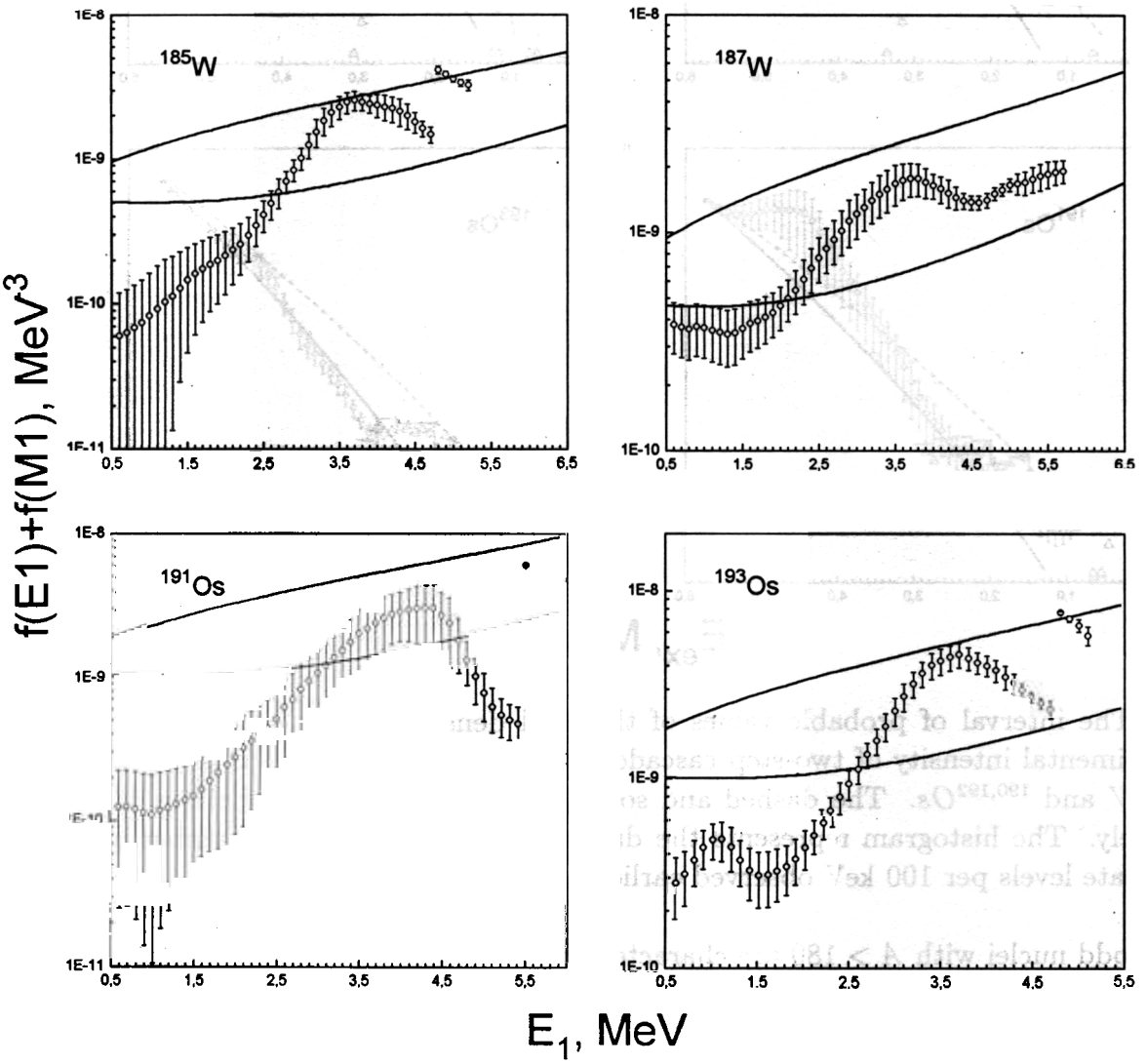

Fig. 3. The probable interval of the sum strength functions $f(E1)+f(M1)$ (points with error bars) providing the reproduction of the experimental data. The upper and lower curves represent the extrapolation of the GEDR "tail" into the region below B_n and the prediction of the model [7] for $E1$ transitions in the sum with $f(M1) = const$ values, respectively.

Unfortunately, at present the analysis [2] can be only carried out under the assumption of similar shapes of the energy dependence of strength functions for the primary and sec-

ondary transitions with equal multipolarities. A comparison between the experimental and calculated two-step cascades to different final levels of the investigated nuclei shows that, most probably, this assumption leads to some overestimation of the level density above the energy of several MeV and to underestimation — at low excitations. This fact in conjunction with the circumstance that some part of the cascades cannot be unambiguously placed in the decay scheme results in a discrepancy for the data in Fig. 1 below the excitation energy 2 MeV.

The simplest interpretation of the observed discrepancy between the experiment and models [7,8] can be obtained from the specific shape of the dependence of ρ on E_{ex}. The dependence of ρ on the excitation energy for all of these nuclei demonstrates a step-like structure at the 2 MeV excitation energy and in addition, a similar structure at $\simeq$ 4 MeV. This result agrees with the qualitative predictions [9] by A.Ignatyuk of the step-like dependence of the level density on the excitation energy. The only discrepancy is that the width of the step-like structure in our data is approximately 2 MeV instead of $\simeq$ 1 MeV in [9]. Theoretical notions of A.Ignatyuk are based on the fact that breaking of a nucleon pair requires a certain excitation energy. Each of these damped "steps" are due to the complication of the structure of the wave function by two quasiparticles as the excitation energy increases. From the data shown in Fig. 2 and notions of model [9] it follows that the next structure of the step-like type should be expected at an excitation energy of about 6.5-7.0 MeV, i. e., after the capture of the neutron with an energy of $\approx$ 1 MeV. This means that the estimated interaction cross sections of neutrons with nuclei can include an additional uncertainty. A similar conclusion about the step-like structure of the level density above the neutron binding energy is made in an analysis of the interaction cross section of neutrons with actinides described in details in [10]. The novelty of the suggested methods of analysis [6,7] and the data obtained within these methods assume, naturally, the necessity of further experimental and theoretical studies of the results discussed in present article.

This work was supported by the RFBR Grant N^o 99-02-17863.

References

1. M.I. Svirin, G.N. Smirenkin, Yad. Fiz, **47** (1988) 84
2. E.V.Vasilieva, V.A. Khitrov, A.M.Sukhovoj, Physics of Particles and Nuclei, **31(2)** (2000) 170
3. J. Honzátko et al., Nucl. Instr. and Meth. **A376** (1996) 434
4. Yu.P. Popov, A.M. Sukhovoj, V.A. Khitrov, Yu.S. Yazvitsky, Izv. AN SSSR, Ser.Fiz. **48** (1984) 1830
5. S.T. Boneva, V.A. Khitrov, A.M. Sukhovoj, A.V. Vojnov, Z. Phys. **A338** (1991) 319
   S.T. Boneva, V.A. Khitrov, A.M. Sukhovoj, A.V. Vojnov, Nucl. Phys. **A589** (1995) 293
6. A.M. Sukhovoj, V.A.Khitrov, Yad. Fiz. **62(1)** (1999) 24
7. S.G. Kadmenskij, V.P. Markushev, W.I. Furman, Sov. J. Nucl. Phys. **37** (1983)165
8. W. Dilg, W. Schantl, H. Vonach, Nucl. Phys. **A217** (1973) 269
9. A.V. Ignatyuk, Report IAEA INDC-233(L), IAEA, Vienna 1985
10. V.M.Maslov, Phys. of Atomic Nuclei **63(2)** (2000) 161

WEEKLY CYCLES OF ELEMENT POLLUTANTS IN AIR OF THE GREATER CAIRO AREA (EGYPT) STUDIED BY NEUTRON ACTIVATION ANALYSIS

M.V. Frontasyeva, A.B. Ramadan*, T.Ye. Galinskaya

Frank Laboratory of Neutron Physics, Joint Institute for Nuclear Research, Dubna, Russia
** National Center for Nuclear Safety and Radiation Control, Cairo, Egypt*

Why is the weather different in working days and in week-ends? Why is it gloomy during the holidays? This variability, noted by Canadian and United States inventories [1] and later nicknamed the "Sunday effect" [2], is characterized by high late-week pollution levels as opposed to the early week levels. According to the interpretation of numerous data offered by American scientists studying the weekly cycles of air pollutants, precipitation, and tropical cyclones in the coastal Atlantic region of the USA, it is connected to a greater extent, with human activity rather than natural phenomena.

As an example of curiosity, the cyclic anthropogenic impact on air pollution in the Greater Cairo Area of Egypt is demonstrated in our work. It is based on the results of elemental analysis of limited number of air filters used to study air pollution in the Greater Cairo Area, a densely populated and industrial district of Egypt. This area differs from the above-mentioned region of the USA not only by its climatic conditions, but also by its week-ends, corresponding in the Arabic world to Thursday and Friday! As well as high concentration of anthropogenic aerosols have been identified over the North Atlantic Ocean [3] associated with the urbanised eastern seaboard of North America, we have noted that Cairo with its suburbs (the Greater Cairo Area), a megapolice encompassing 16 million people, produces a strong weekly pollution cycle.

Results for a total of 30 elements are reported, including lead, cadmium and copper determined by total reflection fluorescence analysis (TXRF) at NCNSRC, Cairo, Egypt.

A seven-day cycle was revealed, with the last two days of the week for the Arabic world (Tuesday-Wednesday) experiencing the highest values of pollutants and with the lowest values associated with the beginning of the week (Saturday-Sunday). It is an excellent extra testing of a hypothesis of weekly cycles of air pollutants, along with precipitation, and tropical cyclones. The weekly cycles of air pollution noted in our work for the Arabic world with its week-ends on Thursday-Friday *(Fig. 1)* are in good agreement with a similar behavior of air pollution in the Christian world with its week-ends on Saturday-Sunday [1].

A pronounced increase of major and trace element concentrations, including heavy metals, rare earth elements and actinides along the valley with the prevailing wind direction, from the north to the south of the Greater Cairo Area was observed in the period under examination *(Fig. 2)*.

The air filters were collected in winter months December-January of 1997-1998 at three aerosol stations located in the north-south direction of 27 km. Total particulate suspended matter has been sampled with high-volume samplers operating at a flow of about 25 m^3/h by pumping 540 m^3 of air through Whatman-41 cellulose filters of 25 x 25 cm in size. Initially measured for the man-made and natural radionuclides, filters then were subdivided, and part of the material was subject to instrumental neutron activation analysis using epithermal neutrons (ENAA) at IBR-2 pulsed fast reactor in Dubna, Russia. Neutron flux density and temperature in the channels of irradiation of the pneumatic system REGATA are shown in *Table 1*. One should note that the high fluxes of epithermal and fast neutrons of IBR-2 reactor are especially favorable for determination of the radionuclides with large resonance integrals.

Table 1. Characteristics of the irradiation channels

Irradiation site	$\phi_{th}x10^{12}$ (n/cm^2s) E=0.55eV	$\phi_{epi}x10^{12}$ (n/cm^2s) E=0.55÷10^5eV	$\phi_{fast}x10^{12}$ (n/cm^2s) E=0.1÷25MeV	$<E_{fast}>$MeV (n/cm^2s) E=0.1÷25MeV	Tempe-rature, °C
Ch1 Cd coated	0.023	3.31	4.32	0.88	70
Ch2	1.23	2.96	4.10	0.92	60

Short-lived radionuclides were determined using small parts of filters (2.5 x 2.5 cm) which were irradiated in channel 2. Long-lived radionuclides were determined using activation with the epithermal neutrons in channel 1.

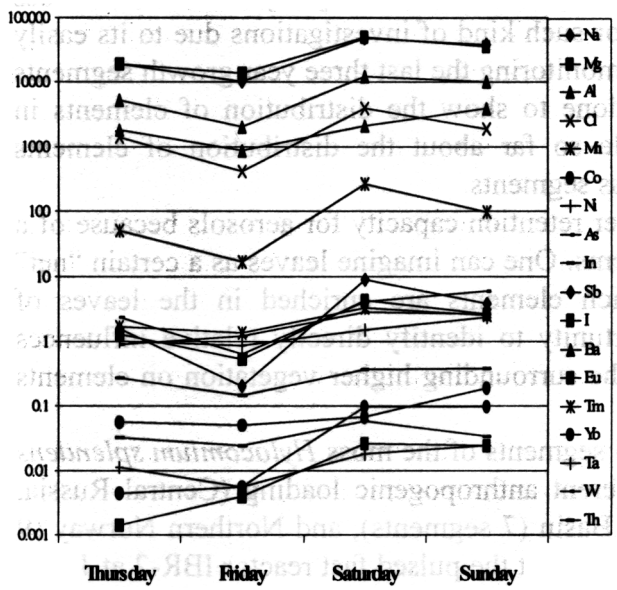

Fig. 1. Irregularity of aerosol elemental content of the South of the Greater Cairo Area

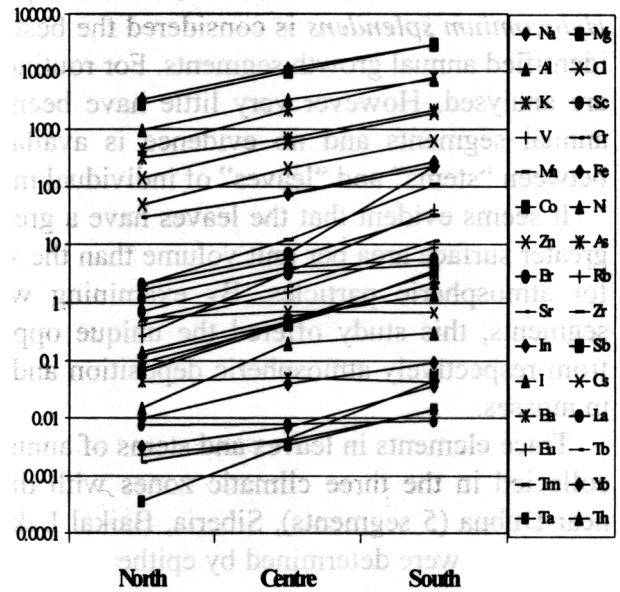

Fig. 2. The Greater Cairo Area aerosol elemental content.

Further investigations will allow us to create coloured geographical maps of temporal and spatial air pollution patterns for the examined periods of time.

This pilot study showed the possibility of obtaining information on air pollution elements using segments of the same air filters exposed for radionuclide determination at the National Center for Nuclear Safety and Radiation Control in Cairo.

REFERENCES

[1] CERVENY, R.S., BALLING, R.C., Jr. Weekly cycles of air pollutants, precipitation and tropical cyclones in the coastal NW Atlantic region. Nature, 394/6, 561- 563 (1998).

[2] GRAEDEL, T.E., FARROW, L.A., WEBER, T.A. Photochemistry of the "Sunday Effect". Environ. Sci. Technol. 11, 690-694 (1977).

[3] ANDERSON, B.E. et al. The impact of U.S. continental outflow on ozone and aerosol distributions over the Western Atlantic. J. Geophys. Res. 98(D12), 23477-23489 (1993).

STUDY OF TRACE ELEMENTS IN ANNUAL SEGMENTS OF MOSS BIOMONITORS USING EPITHERMAL NEUTRON ACTIVATION ANALYSIS: LINK WITH ATMOSTHERIC AEROSOL

Ye.V. Yermakova, M.V. Frontasyeva, E. Steinnes*, K. A. Rahn**

Joint Institute for Nuclear Research, Dubna, Russia
**Norwegian University of Science and Technology, Trondheim, Norway*
***University of Rhode Island, Centre for Atmospheric Chemistry Studies, Narragansett, USA*

Analysis of naturally growing moss as biomonotor is a well established technique for surveying deposition of metals from atmospheric pollution sources [1-3]. The feather moss *Hylocomium splendens* is considered the best for such kind of investigations due to its easily identified annual growth segments. For routine monitoring the last three year growth segments are analysed. However very little have been done to show the distribution of elements in annual segments and no evidence is available so far about the distribution of elements between "stems" and "leaves" of individual moss segments.

It seems evident that the leaves have a greater retention capacity for aerosols because of a greater surface area per unit volume than the stems. One can imagine leaves as a certain "net" for atmospheric particles. By examining which elements are enriched in the leaves of segments, this study offered the unique opportunity to identify directly relative influences from respectively atmospheric deposition and the surrounding higher vegetation on elements in mosses.

Trace elements in leaves and stems of annual segments of the moss *Hylocomium splendens* collected in the three climatic zones with different anthropogenic loading (Central Russia, near Dubna (5 segments), Siberia, Baikal Lake Basin (7 segments), and Northern Norway (9 segments)) were determined by epithermal activation at the pulsed fast reactor IBR-2 at JINR, Dubna.

Data obtained for 32 elements (Na, Mg, AL, Cl, K, Ca, Sc, V, Cr, Mn, Fe, Co, Ni, Zn, As, Br, Rb, Sr, Mo, Cd, Sb, I, Cs, Ba, La, Ce, Sm, Hf, Ta, W, Th, U) were used for the analysis of the inter-annual variations of elemental concentrations in leaves and stems of annual segments.

The major finding is that even through concentrations of elements varied considerably over leaves and stems, leaves/stem ratios for individual segments varied so little that they could be considered characteristic for each element. Plots of elemental concentrations of paired moss leaves and stems from all three places (Central Russia, Siberia, and Northern Norway) showed clearly that the grouping of elements is systematic and geochemically meaningful: elements with the highest leaves/stem ratios are those typically associated with atmospheric aerosol or deposition (lithophilic and chalcophilic elements such as Al, Sc, V, and Sb), whereas elements with the lowest leaves/stem ratios are those typically linked with plant material (K, Zn, Rb, Cs). Intermediate elements with mixed properties are those enriched in plants but also in the atmosphere (Mn, Ca, Mg, Ba, etc.) (**Fig. 1**).

By examining which elements are enriched in the leaves of segments, this study allows one to identify relative atmospheric/plant influences on elements in moss directly, assuming that leaves have a greater effect from aerosol because of a greater surface area per unit volume than stems. The observed grouping of elements (**Fig. 1**) is consistent with this picture: the

"atmospheric" Al-group is enriched in leaves, the "plantlike" K-group is enriched in stems, and the "mixed" Mn-group shows similar concentrations in leaves and stems.

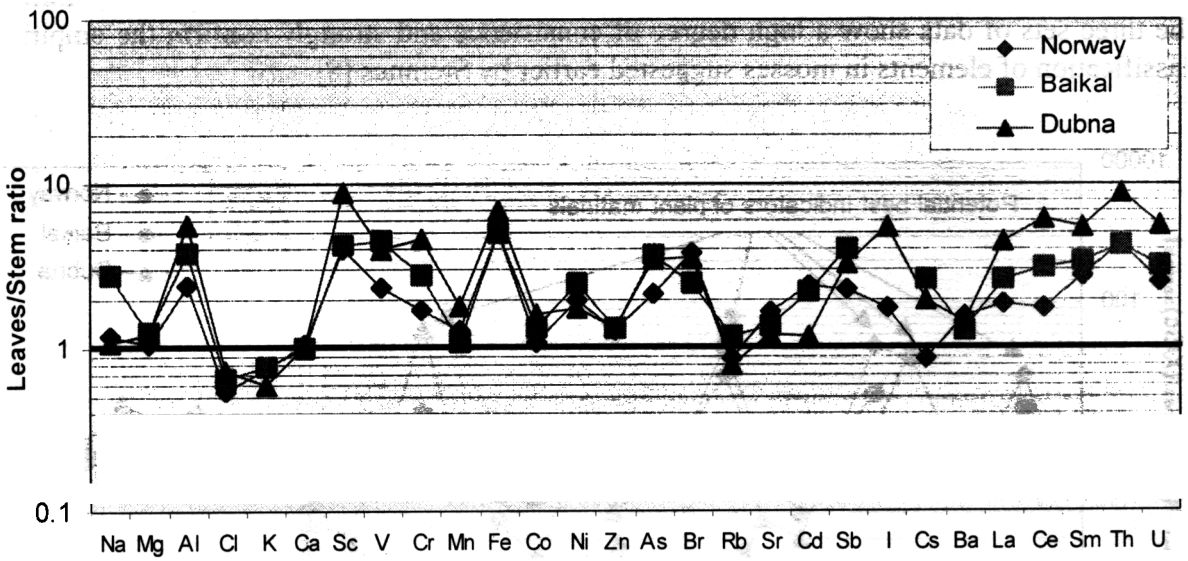

Fig.1. Mean Leaves/Stem ratio of element concentrations

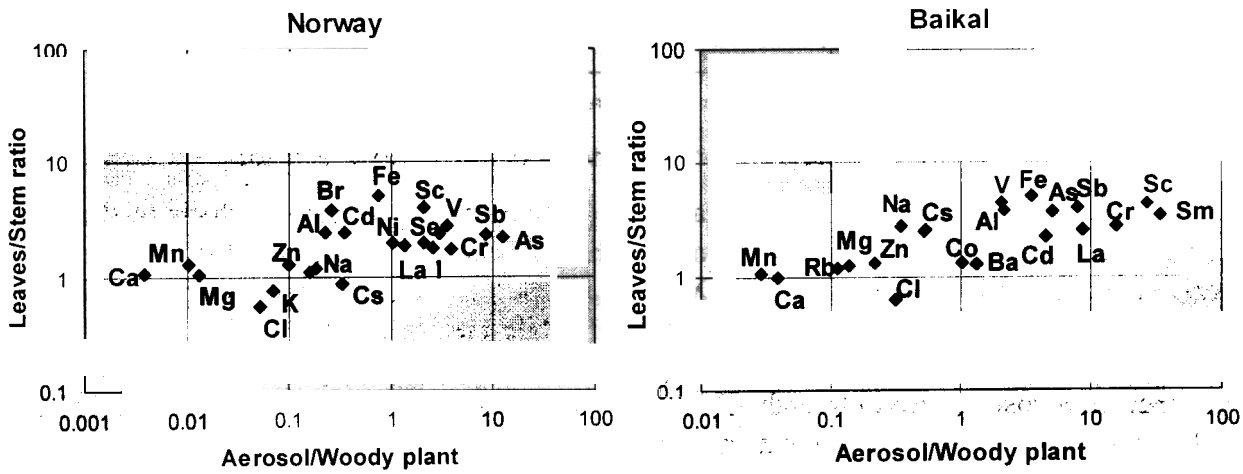

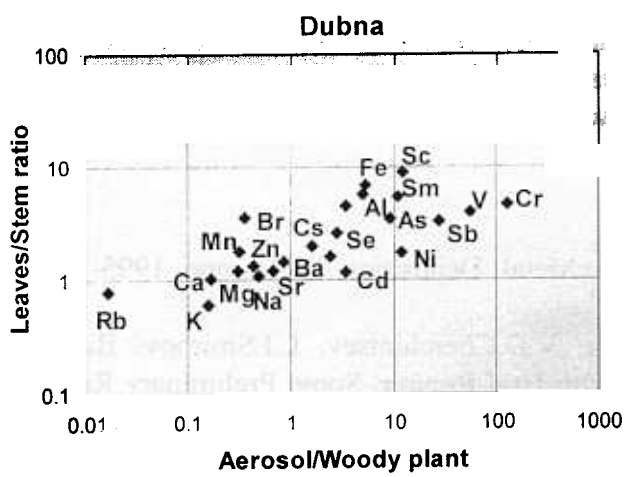

Fig.2. Leaves/Stem ratio in moss versus aerosol/plant ratio

To test these groups further, an independent index of atmospheric/plant ratios (Aerosol/Woody plant) was calculated for the elements concerned and compared with the leaves/stem ratios in the moss (**Fig. 2**) using literature data for aerosols from Moscow (4), Baikal (5) and Norway (6), and Bowen's global averages for woody plants (7). The degree of correlation between the two ratios is remarkable. The three plots in **Fig. 2** show that only a few of the many elements determined in mosses are pure atmospheric

indicators. They are found at the upper right end of the plot, and include V, Cr and Sb, and possibly some other pollution and crustal elements. For elements found between the lower left and the middle of the plot mosses are not satisfactory as indicators of atmospheric pollution. The three sets of data show a high degree of consistence and strongly confirm the empirical classification of elements in mosses suggested earlier by Steinnes [8].

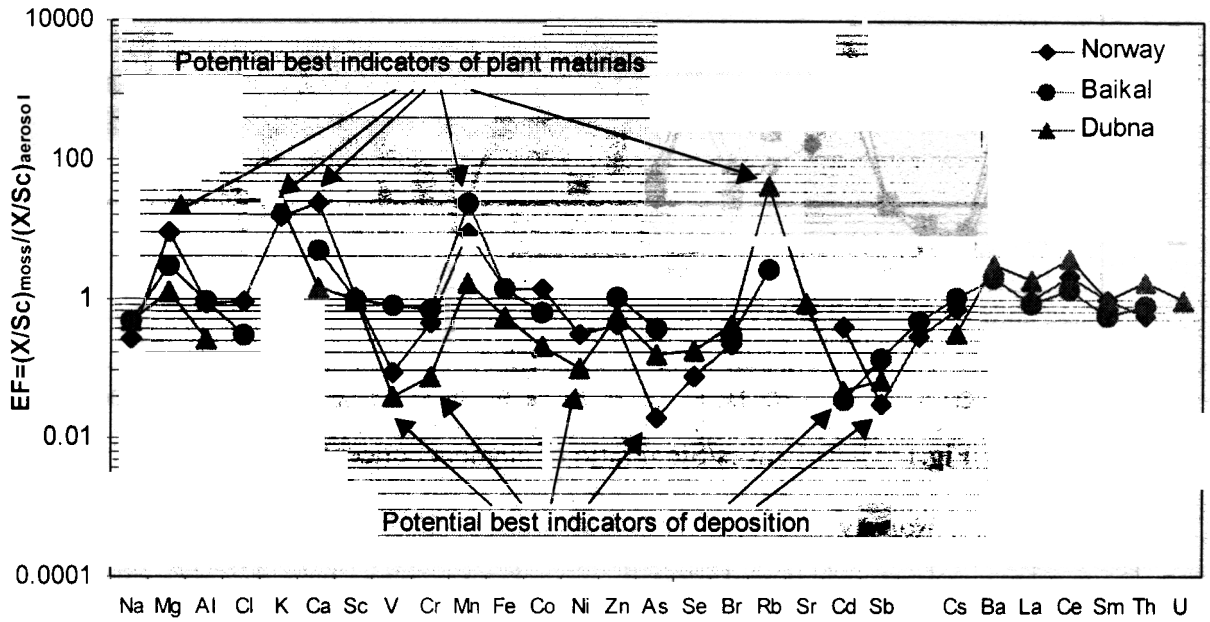

Fig 3. Enrichment factor of elements in moss versus aerosol

Potential best indicators of plant materials (non-crust origin) can be distinguished by comparing the moss average composition with that of atmospheric aerosol (**Fig. 3**). Here the enrichment factor X is defined as $EF=(X/Sc)_{moss}/(X/Sc)_{urban\ aerosol}$. In this plot purely crustal elements not enriched in plants will plot at EF=1 while elements with EF<1 predominate in the relevant aerosol. Since atmospheric deposition of an element is clearly connected to its presence in aerosols, elements with EF<<1 in **Fig. 3** can be considered as good pollution indicators. The potential best indicators of atmospheric pollution as indicated from **Fig. 3** are thus: for Norway V, Ni, As and Sb; for the Baikal Lake Basin Cl (emission from the Baikalsk Cellulose-Paper Plant), Cd and Sb; and for Dubna V, Cr, Co, Ni, As, Cd and Sb. It should be noted that elements showing extremely low EF values in the plot are typically those that have a pollution origin and at the same time show a low retention capacity in the moss.

References

Å.Rühling, E.Steinnes. Atmospheric Heavy Metal Deposition in Europe 1995-1996. *NORD Environment*, 1998:15, 67 p.

2. M.V.Frontasyeva, E.Steinnes, S.M.Lyapunov, V.D.Cherchintsev, L.I.Smirnov. Biomonitoring of Heavy Metal Deposition in the South Ural Region: Some Preliminary Results obtained by Nuclear and Related Techniques, *J.Radioanal.Nucl.Chem.*, Vol.245, No.2 (2000) 415-420.

3. M.V.Frontasyeva, Ye.V.Yermakova, E.Steinnes. Reliability of Mosses (*Hylocomium Splendens*, *Pleurozium Schreberi* and *Calliergon Geganteum*) as Biomonitors of Heavy Metal Atmospheric Deposition in Central Russia. *FLNP JINR Annual Report-1999*, 2000-81, p. 178-180, 2000.
4. A.A.Volokh. Experience in Controlling Air Pollution with Metals and Organic Compounds in Urban and Background Territories. In Geochemical Investigations of Towns' Aglomerations. "Minpriroda", Moscow, 1998, p.40-58 (in Russian).
5. K.A.Rahn, T.V.Khodzhe, U.Tomza. A Study of Trace Elements in Atmospheric Aerosols of the Eastern Siberia Using Neutron Activation and Synchrotron Radiation X-ray Fluorescence Analysis, *Nuclear Instruments and Methods in Physics Research*, A 448, 2000 p. 413-418.
6. K.A.Rahn. The Chemical Composition of the Atmospheric Aerosol. *Technical Report*, Graduate School of Oceanography, University of Rhode Island, 1976, 265 p.
7. H.J.M. Bowen: Environmental Chemistry of the Elements, pp.92-93, Academic Press, London 1979.
8. E.Steinnes. Aspects of Biomonitoring Air Pollutants Using Mosses. In "Plants as Biomonitors. Indicators for Heavy Metals in the Terrestrial Environment". VCH, Weinheim,1993, p.381-394.